

MPC and DOb-based Robust Optimal Control of a New Quadrotor Manipulation System

Ahmed Khalifa¹, Mohamed Fanni² and Toru Namerikawa³

Abstract—This paper introduces motion control scheme of a new aerial manipulation system that consists of 2-link manipulator attached to the bottom of a quadrotor. This new system presents a solution for the limitations found in the current quadrotor manipulation systems. It is very attractive for a wide range of applications due to their unique features. However, control of such system is quite challenging because it is naturally unstable, has strong nonlinearities and couplings, has fast dynamics, is very susceptible to parameters variations due to carrying a payload besides the external disturbances like wind, and has actuator limitations. A robust optimal linear control scheme is proposed to address these issues. The proposed control scheme is based on a hybrid linear Model Predictive Control (MPC) and linear Disturbance Observer (DOb) techniques. The motivation for using DOb is to provide the robustness against the nonlinearities/uncertainties. In addition, it allows one to solve the control problem relying on a set of linear decoupled SISO system which are not affected by nonlinear/uncertain terms. To deal with the actuators' constraints and achieve an optimal controller efforts, a standard MPC will be used. The resulting control scheme is characterized by a low computational load with respect to conventional nonlinear robust solutions. Stability analysis of the proposed control system is presented. The controller is tested to achieve of a point-to-point task space control, under the effect of picking/placing a payload, changing the operating region, and measurement noise. System simulation is implemented in MATLAB/SIMULINK environment with real system parameters, to better emulate a realistic set up. Simulation results enlighten the effectiveness of the proposed control technique.

I. INTRODUCTION

Quadrotor is one of the Unmanned Aerial Vehicles (UAVs) which offer possibilities of speed and access to regions that are otherwise inaccessible to ground robotic vehicles. Quadrotor vehicles possess certain essential characteristics, such as small size and cost, Vertical Take Off and Landing (VTOL), and slow precise movements, which highlight their potential for use in vital applications [1]. Due to their superior mobility, much interest is given to utilize them for mobile manipulation. Several researches has been conducted

¹Ahmed Khalifa is a Research Student at the Department of System Design Engineering, Keio University, Yokohama, Japan. On study leave from Department of Mechatronics and Robotics Engineering, Egypt-Japan University of Science and Technology, Alexandria, Egypt. ahmed.khalifa@ejust.edu.eg

²Mohamed Fanni is with the Department of Mechatronics and Robotics Engineering, Egypt-Japan University of Science and Technology. On leave from Department of Production Engineering and Mechanical Design, Mansoura University, Mansoura, Egypt. mohamed.fanni@ejust.edu.eg

³Toru Namerikawa is with the Department of System Design Engineering, Keio University, Yokohama, Japan. namerikawa@sd.keio.ac.jp

in the area of aerial manipulation [2], [3]. However, the previous introduced systems in the literature that uses a gripper suffers from the limited allowable DOF of the end-effector. Other systems have a manipulator with either two DOF but in certain topology that disables the end-effector to track arbitrary 6-DOF trajectory, or more than two DOF which decreases greatly the possible payload carried by the system. Moreover, the robust control schemes that were presented in the literature for such robots are based on nonlinear controllers which are very complicated and have very high computational cost.

In [4], we propose a new aerial manipulation system that consists of a 2-link manipulator attached to the bottom of a quadrotor. This new system presents a solution for the limitations found in the current quadrotor manipulation systems. Firstly, our proposed aerial manipulator has the capability of manipulating the objects with arbitrary location and orientation because it posses 6-DOF. Secondly, it is based on a minimum manipulator weight for aerial manipulation (2-DOF manipulator). Thirdly, the manipulator provides sufficient and controlled distance between quadrotor and object location.

There are several issues when working with the aerial manipulation systems. The first one is achieving the position holding. In order to achieve this task, a robust control must be implemented such that it can reject uncertainties and disturbances in the system such as wind, payload changes, operation region changes, and measurement noise. The second issue with this system is the limitations of the actuators (thrusters and manipulator motors) which may degrade the performance if it is not considered during controller design. The third issue is the speed of the controller response which must be fast enough to be suitable with the high speed dynamics of the flying robot, so there is a need to design a low computational and fast response control algorithm.

We propose DOb based control technique to achieve the required robustness. The DOb estimate the nonlinear terms and uncertainties then compensates them such that the robotic system acts like a multi-SISO linear systems.

DOb based controller is one of the most popular methods in the field of robust motion control due to its simplicity and computational efficiency. The authors in [5] present the principles of DOb-based control system. In DOb-based robust motion control systems, internal and external disturbances are observed by DOb, and the robustness is simply achieved by feeding-back the estimated disturbances in an inner-loop. Another controller is designed in an outer loop so that the performance goals are achieved without considering

internal and external disturbances. In [6], DOb-based control technique has been applied to robotic systems and showed efficient performance.

Therefore, it is possible to rely on the standard linear MPC methodology to design the controller of the outer loop such that the system performance can be adjusted to achieve desired tracking accuracy and speed, as well as actuators constraints with low computational load and optimal control effort.

Model Predictive Control can represent an appropriate choice to solve this kind of issues partly, providing an optimal control strategy in case of complex constrained dynamical systems [7]. Its application to robotic systems in a true industrial environment, in which disturbances affect the robotic system and the model of the robot is inevitably inaccurate, is still limited. This is due to the high nonlinearity and uncertainties of dynamics in the robotics system. In [8], a nonlinear MPC is utilized to solve the problem of the control of highly nonlinear systems. In [9], robust MPC control design based on feedback linearization and sliding mode control is utilized to achieve trajectory tracking of robotic manipulator. In [10], nonlinear MPC with nonlinear DOb is used to control a robotic system. However, the nonlinear control methods make the MPC to be more complex and has high computational cost which is not suitable to our robotic system.

This paper is organized as follows: In section II, the considered robotic system is described, and kinematic and dynamic analysis are reviewed. The control problem to solve is formulated and the DOb and MPC approaches are described in section III. In section IV, simulation results using MATLAB/SIMULINK are presented. Finally, the main contributions are concluded in section V.

II. DESCRIPTION AND MATHEMATICAL MODELING

3D CAD model of the proposed system is shown in Fig. 1. The system consists mainly of two parts; the quadrotor and the manipulator. Fig. 2 presents a sketch of the proposed system with the relevant frames which indicates the unique topology that permits the end-effector to achieve arbitrary pose. The frames satisfy the Denavit-Hartenberg (DH) convention. The manipulator has two revolute joints. The axis

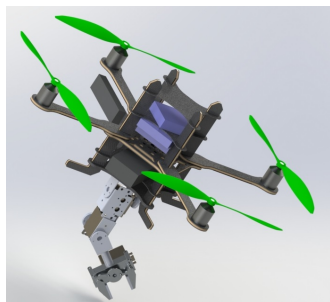


Fig. 1: 3D CAD model of the New Quadrotor Manipulation System

of the first revolute joint (z_0), that is fixed to the quadrotor, is parallel to the body x -axis of the quadrotor (see Fig. 2). The axis of the second joint (z_1) is perpendicular to the axis of the first joint and will be parallel to the body y -axis of quadrotor at home (extended) configuration. Thus, the pitching and rolling rotation of the end-effector is now possible independently from the horizontal motion of the quadrotor. Hence, with this new system, the capability of manipulating objects with arbitrary location and orientation is achieved. By this non-redundant system, the end-effector can achieve 6-DOF motion with minimum number of actuators/links which is an important factor in flight. The proposed system is distinguished from all other previous systems in the literature by having maximum mobility with minimum weight. The quadrotor components are selected such that it can carry a payload equals 500g (larger than the total arm weight and the maximum payload). Asctec pelican quadrotor is used as the quadrotor platform. The maximum thrust force for each rotor is 6N as obtained from an identification process.

The arm components are designed, selected, purchased and assembled such that the total weight of the arm is 200g, has maximum reach in the range between 22cm to 25cm, and can carry a payload of 200g. Three DC motors, (HS-422 (Max torque = 0.4N.m) for gripper, HS-5485HB (Max torque = 0.7N.m) for joint 1, and HS-422 (Max torque = 0.4N.m) for joint 2), are used.

Each rotor j has angular velocity Ω_j and it produces thrust force F_j and drag moment M_j which are given by:

$$F_j = K_{f_j} \Omega_j^2 \quad (1)$$

$$M_j = K_{m_j} \Omega_j^2 \quad (2)$$

where K_{f_j} and K_{m_j} are the thrust and drag coefficients.

Let Σ_b , O_b - x_b y_b z_b , denotes the vehicle body-fixed reference frame with origin at the quadrotor center of mass, see Fig. 2. Its position with respect to the world-fixed inertial reference frame, Σ , O - x y z , is given by the (3x1) vector $p_b = [x, y, z]^T$, while its orientation is given by the rotation matrix R_b :

$$R_b(\Phi_b) = \begin{bmatrix} C(\psi)C(\theta) & S(\psi)S(\theta)C(\phi) - S(\psi)C(\phi) & S(\psi)S(\phi) + C(\psi)S(\theta)C(\phi) \\ S(\psi)C(\theta) & C(\psi)C(\phi) + S(\psi)S(\theta)S(\phi) & S(\psi)S(\theta)C(\phi) - C(\psi)S(\phi) \\ -S(\theta) & C(\theta)S(\phi) & C(\theta)C(\phi) \end{bmatrix}, \quad (3)$$

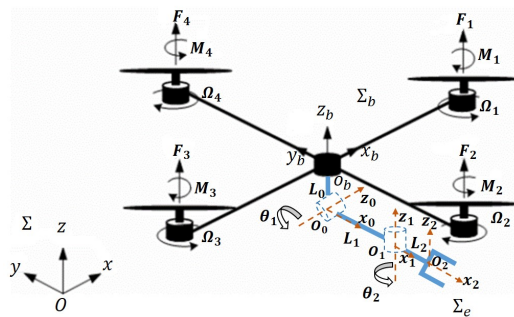


Fig. 2: Schematic of Quadrotor Manipulation System with relevant frames

where $\Phi_b = [\psi, \theta, \phi]^T$ is the triple ZYX yaw-pitch-roll angles. Note that $C(\cdot)$ and $S(\cdot)$ are short notations for $\cos(\cdot)$ and $\sin(\cdot)$. Let us consider the frame Σ_e , O_2 - x_2 y_2 z_2 , attached to the end-effector of the manipulator, see Fig. 2. Thus, the position of Σ_e with respect to Σ is given by

$$p_e = p_b + R_b p_{eb}^b, \quad (4)$$

where the vector p_{eb}^b describes the position of Σ_e with respect to Σ_b expressed in Σ_b . The orientation of Σ_e can be defined by the rotation matrix

$$R_e = R_b R_e^b, \quad (5)$$

where R_e^b describes the orientation of Σ_e w.r.t Σ_b .

In [4], the equations of motion of the proposed robot have been derived in details. The dynamical model of the quadrotor-manipulator system can be written as follows:

$$M(q)\ddot{q} + C(q, \dot{q})\dot{q} + G(q) + d_{ex} = \tau; \quad \tau = Bu \quad (6)$$

where $q = [x, y, z, \psi, \theta, \phi, \theta_1, \theta_2]^T \in R^8$ is the vector of the generalized coordinates, $M \in R^{8 \times 8}$ represents the symmetric and positive definite inertia matrix of the combined system, $C \in R^{8 \times 8}$ is the matrix of Coriolis and centrifugal terms, $G \in R^8$ is the vector of gravity terms, $d_{ex} \in R^8$ is the vector of the external disturbances, $\tau \in R^8$ is the vector of the generalized input torques/forces, $u = [F_1, F_2, F_3, F_4, \tau_{m_1}, \tau_{m_2}]^T$ is the vector of the actuator inputs, $B = HN$ is the input matrix which is used to generate the body forces and moments from the actuator inputs.

III. CONTROLLER DESIGN

This section presents the proposed motion control strategy and DOb based control. Fig. 3 presents the functional block diagram of the proposed control system. In this control strategy, the system nonlinearities, uncertainties, external disturbances, τ^{dis} , are treated as disturbances which will be estimated, $\hat{\tau}^{dis}$, and canceled by the DOb in the inner loop. The system can be now considered as linear SISO plants and thus the MPC is used in the external loop to achieved the objective response for the system by producing τ^{des} .

A. Disturbance Observer Loop

A block diagram of the DOb inner loop is shown in Fig. 4. In this figure, $M_n \in R^{8 \times 8}$ is the system nominal inertia matrix, τ and τ^{des} are the robot and desired inputs, respectively, $P = diag([g_1, \dots, g_i, \dots, g_8])$ with g_i is the bandwidth of the

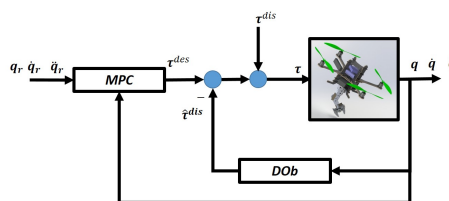


Fig. 3: Functional block diagram of the proposed control system

i^{th} variable of q , $Q(s) = diag([\frac{g_1}{s+g_1}, \dots, \frac{g_i}{s+g_i}, \dots, \frac{g_8}{s+g_8}]) \in R^{8 \times 8}$ is the matrix of the low pass filter of DOb. The velocity is estimated by using a low pass filter, $Q_v(s) = diag([\frac{g_{v1}}{s+g_{v1}}, \dots, \frac{g_{vi}}{s+g_{vi}}, \dots, \frac{g_{v8}}{s+g_{v8}}]) \in R^{8 \times 8}$, and with cut-off frequency of $P_v = diag([g_{v1}, \dots, g_{vi}, \dots, g_{v8}])$ (i.e. precise velocity measurement is achieved in a predetermined bandwidth). τ^{dis} represents the system disturbances including the Coriolis, centrifugal and gravitational terms, and $\hat{\tau}^{dis}$ represents the system estimated disturbances.

The system disturbance τ^{dis} can be assumed as:

$$\begin{aligned} \tau^{dis} &= (M(q) - M_n)\ddot{q} + \tau^d; \\ \tau^d &= C(q, \dot{q})\dot{q} + G(q) + d_{ex} \end{aligned} \quad (7)$$

Substituting from (7), then (6) can be rewritten as:

$$M_n\ddot{q} + \tau^{dis} = \tau \quad (8)$$

Now if the disturbance observer performs optimally, that is $\hat{\tau}^{dis} = \tau^{dis}$, the dynamics from the DOb loop input τ^{des} to the output of the robot manipulator is given by:

$$M_n\ddot{q} = \tau^{des} \quad (9)$$

Since M_n is a diagonal matrix, the system can be treated as multi-decoupled linear SISO systems as following:

$$M_{n_i}\ddot{q}_i = \tau_i^{des}, \quad (10)$$

or simply in the acceleration space as:

$$\ddot{q}_i = \ddot{q}_i^{des} \quad (11)$$

The control input, τ , in Fig. 4 can be calculated as:

$$\begin{aligned} \tau &= \frac{1}{(1 - Q(s))}[M_n\ddot{q}^{des} - Q(s)M_n\ddot{q}] \\ &= M_n\ddot{q}^{des} + M_nP e_v; \quad e_v = \dot{q}^{des} - \dot{q} \end{aligned} \quad (12)$$

This control law leads to the following error dynamics:

$$\begin{aligned} M(q)\dot{e}_v + C(q, \dot{q})e_v + K_v e_v &= \delta; \\ K_v &= P M_n \end{aligned} \quad (13)$$

where

$$\begin{aligned} \delta &= \Delta M(q)\ddot{q}^{des} + C(q, \dot{q})\dot{q}^{des} + G(q) + d_{ex}; \\ \Delta M(q) &= M(q) - M_n, \end{aligned} \quad (14)$$

Equation (13) represents the error dynamics of DOb-based robust control of the quadrotor manipulation system.

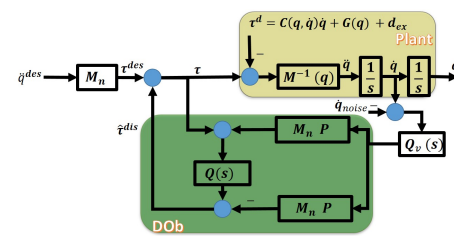


Fig. 4: Block diagram of internal loop (DOb)

To study the inner loop stability, assume the following Lyapunov function:

$$V = \frac{1}{2}e_v^T M(q)e_v + \frac{1}{2}\delta^T \delta \quad (15)$$

The time derivative of this function is:

$$\dot{V} = e_v^T M(q)\dot{e}_v + \frac{1}{2}e_v^T \dot{M}(q)e_v + \delta^T \dot{\delta} \quad (16)$$

Substituting from (13),

$$\dot{V} = e_v^T \delta - e_v^T K_v e_v + \frac{1}{2}e_v^T (\dot{M}(q) - 2C(q, \dot{q}))e_v + \delta^T \dot{\delta} \quad (17)$$

The dynamic equation of motion (6) posses several well known properties [11]. These properties will be used to complete the stability analysis and they are stated as follows:

$$\lambda_{min}\|\nu\|^2 \leq \nu^T M(q)\nu \leq \lambda_{max}\|\nu\|^2 \quad (18)$$

$$\nu^T (\dot{M}(q) - 2C(q, \dot{q}))\nu = 0 \quad (19)$$

where $\dot{M}(q) - 2C(q, \dot{q})$ is a skew-symmetric matrix, $\nu \in R^8$ represents a 8-dimensional vector, and λ_{min} and λ_{max} are positive real constants.

Substituting from (19) into (17) with the assumption that δ changes very slow (i.e. $\dot{\delta} = 0$):

$$\dot{V} = e_v^T \delta - e_v^T K_v e_v \quad (20)$$

From the robot dynamic properties:

$$\begin{aligned} \dot{V} &\leq -\gamma V + \sqrt{\frac{2V}{\lambda_{min}}} |\delta|; \\ \gamma &= \frac{2K_v}{\lambda_{max}} \end{aligned} \quad (21)$$

Thus, the time derivative of the Lyapunov function is smaller than zero and the convergence rate increases proportionally with K_v . However, by inspecting the inner loop, one can find that there is a practical constraint on the choice of K_v due to the usage of the velocity filter. The characteristic equation of the inner loop can be driven as:

$$P_{c_i} = s^2 + g_{v_i}s + \alpha_i g_i g_{v_i}, \quad (22)$$

where, $\alpha_i = \frac{M_{nii}}{M_{ii}}$. The damping coefficient of this equation is $0.5\sqrt{\frac{g_i g_{v_i}}{\alpha_i}}$, which should larger than or equal 0.707 to improve the robustness against both disturbances and noise. Thus, the following inequality should be hold:

$$\alpha_i g_i \leq \frac{g_{v_i}}{2}, \quad (23)$$

Rewrite (23) with respect to K_v ,

$$\frac{K_{v_i}}{M_{ii}} \leq \frac{g_{v_i}}{2}, \quad (24)$$

To sum up, (21) shows that the stability and robustness of the control system is improved by increasing K_v (i.e. by increasing M_n and P) but without violating the robustness constraint in (24).

B. Linear Model Predictive Control

By virtue of the rejection of the nonlinearities, disturbances, uncertainties, and noise through the use of DOB internal loop, the MPC controller have not to consider uncertainties and can designed based on the nominal 8 SISO decoupled models of the system with satisfying the actuators constraints, $u_{min} \leq u \leq u_{max}$.

The SISO model of the system is given by:

$$\begin{aligned} \dot{x}_p(t) &= A_p x_p(t) + B_p u_{mpc}(t) \\ q_i(t) &= C_p x_p(t) \end{aligned} \quad (25)$$

where, $x_p = \begin{bmatrix} x_1 \\ x_2 \end{bmatrix} = \begin{bmatrix} \dot{q}_i \\ q_i \end{bmatrix}$, $A_p = \begin{bmatrix} 0 & 0 \\ 1 & 0 \end{bmatrix}$, $B_p = \begin{bmatrix} 1 \\ 0 \end{bmatrix}$, $C_p = \begin{bmatrix} 0 & 1 \end{bmatrix}$, and $u_{mpc}(t)$ is the output of the MPC which will be \dot{q}^{des} . The general design philosophy of model predictive control is to compute a trajectory of a future manipulated variable $u_{mpc}(t)$ to optimize the future behavior of the plant output $q_i(t)$. The optimization is performed within a limited time window starts by t_i with length T_p . To achieve offset free MPC, it will be designed based on an augmented model of the plant which is given as following:

$$\begin{aligned} \dot{x}(t) &= Ax(t) + Bu_{mpc}(t) \\ q_i(t) &= Cx(t) \end{aligned} \quad (26)$$

$$\text{where, } x(t) = \begin{bmatrix} \dot{x}_p(t) \\ q_i(t) \end{bmatrix}, A = \begin{bmatrix} A_p & O_{2 \times 1} \\ C_p & 1 \end{bmatrix}, B = \begin{bmatrix} B_p \\ 0 \end{bmatrix}, C = \begin{bmatrix} O_{1 \times 2} & 1 \end{bmatrix},$$

The MPC design is based on the solution of the so-called Finite Horizon Optimal Control Problem which consists of minimizing a suitably defined cost function with respect to the control sequence. The cost function is given as:

$$\begin{aligned} J = \int_0^{T_p} (q_r(t_i) - q(t_i + \iota | t_i))^T Q_{mpc} (q_r(t_i) - q(t_i + \iota | t_i)) \\ + \dot{u}_{mpc}^T(\iota) R_{mpc} \dot{u}_{mpc}(\iota) d\iota \end{aligned} \quad (27)$$

where Q_{mpc} and R_{mpc} are weighting matrices that must be positive definite to ensure the stability of the outer loop.

Obtaining the plant response model is a key part of the implementation of an MPC controller. In our design, the controller models the system response based on Laguerre polynomials [12] with parameters; a which is the scaling factor and b is the number of terms. By applying the principle of receding horizon control (i.e., the control action will use only the derivative of the future control signal at $\iota = 0$), one can get the derivative of the optimal control for the unconstrained problem.

The next step is to formulate the constraints as part of design requirements. A simple algorithm, called Hildreth's quadratic programming procedure, was proposed for solving this problem. This method will lead to very simple programming procedures for finding real time optimal solutions of constrained minimization problem.

To ensure the outer loop stability, an exponential weighted cost function [13] is used in which the system matrix, A , is modified to be $(A - \varrho I)$ and Q_{mpc} to $(Q_{mpc} + 2\varrho P_{mpc})$,

where P_{mpc} is the solution of the Riccati equation. The selection of weighting factor, ϱ , is to make sure that the design model with $(A - \varrho I)$ is stable with all eigen values on the left-half of the complex plane.

In order to specify the closed-loop response speed, a new tuning parameter is used β . During solution of Riccati equation, the A matrix is modified to $(A + \beta I)$ and Q_{mpc} to $(Q_{mpc} + 2(\varrho + \beta)P_{mpc})$.

Fig. 5 shows the complete hybrid block diagram of the proposed control system. Since the vehicle (quadrotor) is an under-actuated system, i.e., only 4 independent control inputs are available against the 6 DOF, the position and the yaw angle are usually the controlled variables, while pitch and roll angles are used as intermediate control inputs for horizontal positions control. Therefore, the proposed control system consists from two DOb-based controllers by dividing q in to two parts; one for $\zeta = [x, y, z, \psi, \theta_1, \theta_2]$ (with MPC_ζ , M_{n_ζ} , P_ζ , Q_ζ) and the other for $\sigma_b = [\theta, \phi]$ (with MPC_σ , M_{n_σ} , P_σ , Q_σ). The desired end-effector's pose, $\chi_{e,r}$, is fed to the inverse kinematics algorithm such that the desired vehicle/joint space trajectories $\zeta_r(t)$ are obtained. After that, the controller block receives the desired trajectories and the feedback signals from the system and provides the control signal, τ . The desired values $\sigma_{b,r}$ for the intermediate controller are obtained from the output of position controller, τ_ζ , through the following simplified nonholonomic constraints relation:

$$\sigma_{b,r} = \frac{1}{\tau_\zeta(3)} \begin{bmatrix} C(\psi) & S(\psi) \\ S(\psi) & -C(\psi) \end{bmatrix} \begin{bmatrix} \tau_\zeta(1) \\ \tau_\zeta(2) \end{bmatrix} \quad (28)$$

However, the response of the σ controller must be much faster than that of the quadrotor position controller such that it can track the changes in the position controller. This can be achieved by the tuning parameters of both DOb and MPC, as it is explained previously.

The output of two controllers, τ_ζ and τ_σ , are mixed to generate the final control vector τ which is then converted to the forces/torques applied to quadrotor/manipulator through the following relation:

$$u = B_6^{-1} \begin{bmatrix} \tau_\zeta(1 : 4) \\ \tau_\sigma \\ \tau_\zeta(5 : 6) \end{bmatrix} \quad (29)$$

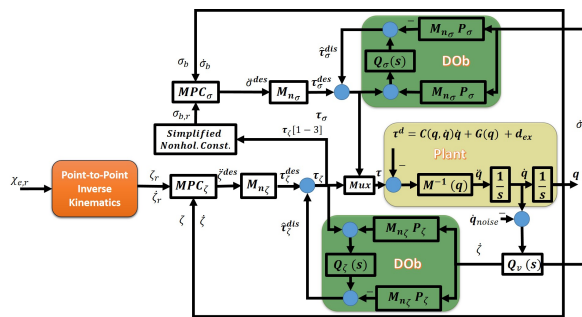


Fig. 5: Block diagram of the detailed control system for the quadrotor manipulation system

where $B_6 \in R^{6 \times 6}$ is part of B matrix and it is given by $B_6 = B(3 : 8, 1 : 6)$.

IV. SIMULATION RESULTS

In this section the previously proposed control system is simulated using MATLAB/SIMULINK program to the model of the considered aerial manipulation robot. Note that the model has been identified on the basis of real data through experimental tests, and a normally distributed measurement noise, with mean of 10^{-3} and standard deviation of 5×10^{-3} , has been added to the measured signals. As a result, the simulation environment is quite realistic. The identified parameters are given in [4].

To achieve task space control, the desired values of end-effector pose (Multi operational regions and point-to-point control) are used to generate the desired trajectories for ζ using the inverse kinematics and then applied to the algorithm for generating the desired trajectories in the quadrotor/joint space which will provide Quintic polynomial trajectories as the reference trajectories. By using these types of trajectories for the joint space control, we can avoid the vibrational modes because they have sinusoidal acceleration.

Parameters of DOb-based control is given in Table I. The controller is tested to stabilize and track the desired

TABLE I: Controller parameters

| Par. | Val. | Par. | Val. |
|----------------------|---------------------------------------------|------------------------|---------|
| M_{n_ζ} | $diag\{1.2, 1.2, 2, 0.5, 0.005, 0.005\}$ | ϱ_{mpc_ζ} | 10 |
| M_{n_σ} | $diag\{0.5, 0.5\}$ | Q_{mpc_ζ} | $C^T C$ |
| u_{max} | $[6, 6, 6, 6, 0.7, 0.4]^T$ | Q_{mpc_σ} | $C^T C$ |
| u_{min} | $[0, 0, 0, 0, -0.7, -0.4]^T$ | R_{mpc_ζ} | I_6 |
| P_ζ | $diag\{2.4, 2.4, 14.5, 0.6950, 19.5, 4.5\}$ | R_{mpc_σ} | I_2 |
| P_σ | $diag\{1.3, 0.76\}$ | ϱ_{mpc_σ} | 15 |
| β_{mpc_ζ} | 5 | T_p | 70 |
| β_{mpc_σ} | 10 | b | 6 |
| g_{v_i} | 100 | a | 0.6 |

quadrotor/joint space trajectories under the effect of picking a payload of value 150g at instant 15s and placing it at instant 55s. The simulation results in quadrotor/joint space are presented in Fig. 6. Fig. 7 shows response of system in the task space (the actual end-effector position and orientation can be found from the forward kinematics). These results show that the proposed motion control scheme is able to track the desired trajectories, with achieving the control objectives. Figs. 8 shows the control effort, the required thrust forces and manipulator torques, which are in the allowable limits.

V. CONCLUSION

The problem of the motion control of a new aerial manipulation robot called "Quadrotor Manipulation System" is presented. This robot has several issues in point of view the control system which have been addressed in this paper. Description and mathematical modeling of the proposed system are presented. Hybrid linear DOb/MPC based control design is proposed as a motion control system. The DOb loop is used to enforce robust linear input/output behavior

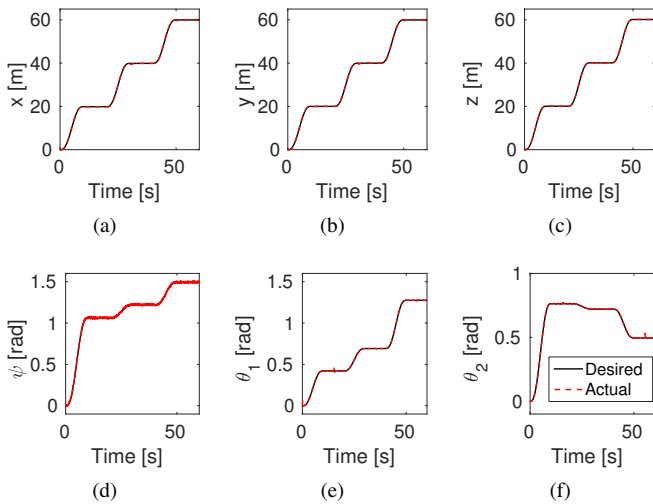


Fig. 6: The actual response of the Quadrotor/ Manipulator variables: a) x , b) y , c) z , d) ψ , e) θ_1 , and f) θ_2

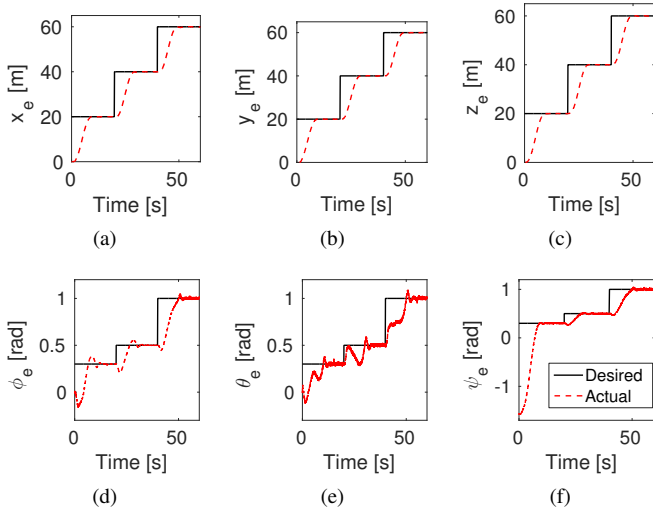


Fig. 7: The actual response of the end-effector position and orientation: a) x_e , b) y_e , c) z_e , d) ϕ_e , e) θ_e , and f) ψ_e

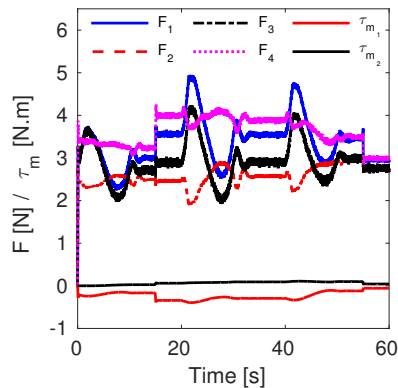


Fig. 8: The required controller efforts

of the plant by canceling disturbances, measurement noise,

and plant/model mismatch. After that the MPC controller is used in the external loop to achieve the required closed loop performance and control objectives with low computational load. The stability grandee is proved for this controller. The controller is tested to achieve trajectory tracking under the effect of picking/placing a payload, changing the operating region, and the measurement noise. The system is simulated using MATLAB/SIMULINK based on real parameters. Simulation results indicate the efficiency of the proposed controller.

ACKNOWLEDGMENT

The first author is supported by a scholarship from the Mission Department, Ministry of Higher Education of the Government of Egypt which is gratefully acknowledged.

REFERENCES

- [1] S. Gupte, P. I. T. Mohandas, and J. M. Conrad, "A survey of quadrotor unmanned aerial vehicles," in *Southeastcon, 2012 Proceedings of IEEE*. IEEE, 2012, pp. 1–6.
- [2] S. Kim, S. Choi, and H. J. Kim, "Aerial manipulation using a quadrotor with a two dof robotic arm," in *Intelligent Robots and Systems (IROS), 2013 IEEE/RSJ International Conference on*. IEEE, 2013, pp. 4990–4995.
- [3] G. Heredia, A. Jimenez-Cano, I. Sanchez, D. Llorente, V. Vega, J. Braga, J. Acosta, and A. Ollero, "Control of a multirotor outdoor aerial manipulator," in *Intelligent Robots and Systems (IROS 2014), 2014 IEEE/RSJ International Conference on*. IEEE, 2014, pp. 3417–3422.
- [4] A. Khalifa, M. Fanni, A. Ramadan, and A. Abo-Ismail, "Modeling and control of a new quadrotor manipulation system," in *2012 IEEE/RAS International Conference on Innovative Engineering Systems*. IEEE, 2012, pp. 109–114.
- [5] S. Li, J. Yang, W.-h. Chen, and X. Chen, *Disturbance observer-based control: methods and applications*. CRC Press, 2014.
- [6] E. Sarıyıldız, H. Yu, K. Yu, and K. Ohnishi, "A nonlinear stability analysis for the robust position control problem of robot manipulators via disturbance observer," in *Mechatronics (ICM), 2015 IEEE International Conference on*. IEEE, 2015, pp. 28–33.
- [7] L. Magni and R. Scattolini, "Model predictive control of continuous-time nonlinear systems with piecewise constant control," *Automatic Control, IEEE Transactions on*, vol. 49, no. 6, pp. 900–906, 2004.
- [8] T. Hatanaka, T. Yamada, M. Fujita, S. Morimoto, and M. Okamoto, "Nonlinear model predictive control towards new challenging applications," *Nonlinear Model Predictive Control Towards New Challenging Applications*, vol. 384, pp. 561–569, 2009.
- [9] A. Ferrara, G. P. Incremona, and L. Magni, "A robust mpc/ism hierarchical multi-loop control scheme for robot manipulators," in *Decision and Control (CDC), 2013 IEEE 52nd Annual Conference on*. IEEE, 2013, pp. 3560–3565.
- [10] C. Liu, W. Chen, and J. Andrews, "Trajectory tracking of small helicopters using explicit nonlinear mpc and dobc," in *18th IFAC World Congress, IFAC WC, Milano, Italy*, vol. 18, 2011, pp. 1498–1503.
- [11] P. J. From, J. T. Gravdahl, and K. Y. Pettersen, *Vehicle-Manipulator Systems*. Springer, 2014.
- [12] T. Barry and L. Wang, "A model-free predictive controller with laguerre polynomials," in *Control Conference, 2004. 5th Asian*, vol. 1. IEEE, 2004, pp. 177–184.
- [13] L. Wang, *Model predictive control system design and implementation using MATLAB®*. Springer Science & Business Media, 2009.